Effect of infill parameters on mechanical properties in additive manufacturing

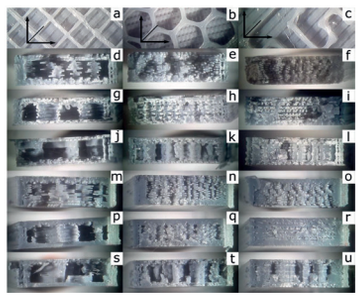

Efecto de los parámetros del relleno sobre las propiedades mecánicas en fabricación aditiva

Juan Ivorra-Martinez, Luis Quiles-Carrillo, Diego Lascano, Santiago Ferrandiz and Teodomiro Boronat
Universitat Politècnica de València. Materials Technology Institute. Plaza Ferrándiz y Carbonell, s/n – 03801 Alcoy (Spain)

DOI: http://dx.doi.org/10.6036/9674 | Recibido: 17/02/2020 • Inicio Evaluación: 04/12/2019 • Aceptado: 18/03/2020

RESUMEN

- El propósito de este trabajo es estudiar y esbozar los efectos de los parámetros del relleno (porcentaje y patrón) de la fabricación por deposición fundida sobre las propiedades mecánicas de probetas de PLA.
  Se han analizado tres patrones de relleno (rectilíneo, panal de abeja y curva Hilbert), y tres porcentajes de relleno distintos (20, 60 y 90 por ciento). Las propiedades examinadas fueron resistencia a la tracción, módulo de tracción, alargamiento, tenacidad utilizando ensayo Charpy, morfología de las fracturas de los ensayos de tracción e impacto y análisis termomecánico. Además, se realizó un análisis térmico utilizando calorimetría diferencial de barrido al polímero virgen para determinar la temperatura de procesamiento.
  Los resultados mostraron la influencia de los parámetros de llenado en la impresión 3D sobre las propiedades mecánicas de la pieza obtenida. El patrón de llenado influye en gran medida en las propiedades mecánicas de las piezas con bajos porcentajes de relleno. El patrón de relleno de panal de abeja es el que tiene mejores resultados mecánicos de los tres analizados.
  La geometría del patrón de relleno también influye sobre el tiempo de procesado. Los cambios de dirección de las boquillas en patrones complejos alargan el tiempo de procesamiento.
  Los resultados obtenidos pueden influir significativamente en el diseño y la fabricación de piezas a medida mediante el modelado de la deposición de material fundido.
- **Palabras clave:** Fabricación aditiva, modelado de deposición en fundido, porcentaje de relleno, patrón de relleno, PLA.

ABSTRACT

The purpose of this paper is to study and outline the effects of infill parameters (percentage and pattern) using fused deposition manufacturing on mechanical properties of PLA printed samples. Three infill patterns were tested (rectilinear, honeycomb and Hilbert curve) while infill percentage was tested at three levels (20, 60 and 90 per cent). The properties examined were tensile strength, tensile modulus, elongation, Charpy impact test, morphology of the fractures of tensile and impact test and thermo mechanical analysis. Also, a thermal analysis was done using differential scanning calorimetry to the raw polymer in order to determine the processing temperature. Results showed the influence of the filling parameters in 3D printing on the mechanical properties of the obtained part. The filling pattern greatly influences the mechanical properties of parts with low filling percentages. Honeycomb filling pattern is the one with better mechanical results. The complexity of the filling pattern influences on the processing time. Nozzle direction changes in complex patterns lengthening processing time. Results can significantly influence custom design and manufacturing of parts using material fused deposition modeling.

Keywords: Additive manufacturing, fused deposition modelling, infill percentage, infill pattern, PLA.

1. INTRODUCTION

Additive Manufacturing (AM), also known as 3D printing, has attracted attention for the manufacture of solids free form manufacturing (SFF) systems with increased competitiveness. The most common technique of AM is Fused Deposition Modelling (FDM), in which a thermoplastic material is heated to a semi-fused state and then extruded as an ultrafine filament, layer by layer, to construct a three-dimensional object following the trajectories defined in a computer-aided design data file.

Initially this technique provided designers with a tool to quickly generate an initial prototype of their ideas as 3D printing greatly simplifies prototype production regardless of mechanical properties, only appearance mattered [1, 2]. AM allows to reduce design and manufacturing processes from weeks to a few hours, allowing to innovate on the fly [3, 4]. In this way, efficiency can be increased, and production costs reduced in the manufacturing sector [5, 6].

But now any application can be tackled, the FDM process has been recognized as a reliable and an economical technique to be used in a large number of applications in various fields. Personalization of FDM manufactured parts has allowed the biomedical area to benefit from this processing technique, these include the manufacture of orthoprosthetic devices [7], dentistry [8], scaffolds [9], even parts as sensitive as cardiovascular stents [10]. Parts obtained by AM can also be used for practical applications, in which case they must withstand various amounts of mechanical and environmental stresses during its use. Therefore, it is important to know the required loading conditions and the physical properties of AM manufactured parts should be similar to those obtained by traditional processes such as injection [11, 12].

The quality and mechanical properties of a product manufactured by FDM depend on a large number of parameters whose combination is complex to understand [13, 14]. These parameters that influence the mechanical performance and quality of the parts obtained by FDM can be very diverse, such as the layer thick-

ness, raster angle, air gap, build orientation, feed rate and the filling pattern, among others [14, 15]. The effect on the mechanical of the screw rotation velocity, the slice thickness and the deposition velocity on mechanical properties was analyzed [16]. Other investigations confirm that the properties are highly influenced by the process parameters such as the study of the deposition velocity and the screw rotation influence in terms of road width on the mechanical performance of the parts [17]. Recent studies show that the modelling direction also plays a significant role in the mechanical properties as several authors pointed [18, 19]. The infill density or air gap between the adjacent filaments also plays an important role in mechanical characteristics since the change would affect the bounding degree between two fibers which affects the tensile strength of the product [20]. The importance of filling density was also pointed out by other authors [21, 22], since the parts with higher fill levels have more material and resist stress better. The infill rate shows high influence on the ultimate shear strength compared with other parameters; Its influence is nearly twice the one done by thickness and four times more than heat treatment [21]. Therefore it is necessary to determine the influence of the processing parameters on the mechanical behavior since it is crucial for functional parts [23] and a further investigation on the effect of other printing parameters, such as the type of filling and its density, as bibliology related to this topic is somewhat scarce. The studies of mechanical characteristics of parts obtained by FDM have been especially focused when ABS material has been used [11, 24, 25] while the PLA material used in this study has not been extensively analyzed [9, 24, 26].

The present paper studies on the production process of FDM samples, in the study the effects of the manufacturing parameters are analyzed (infill percentage and filling pattern) on the mechanical and thermomechanical properties of the produced specimens. Several researchers have worked on the effects either of the infill percentage and print orientation, this paper focuses on the infill density and the pattern on a wide range of properties such us mechanical properties, fracture morphology, dynamical-mechanical behavior and thermal properties.

2. TOOLS AND METHODS

2.1. MATERIAL SPECIFICATION

A PLA coil provided by BCN3D (Barcelona, Spain) has been used as raw material for this work, the material characteristics are shown in Table I. Prior to fusing modeling, the filaments were dried at 60 ºC for 24h in oven in order to remove moisture from the surrounding environment. Drying procedure was also applied before mechanical testing in order to prevent inconsistent results among the specimens.

2.2. THERMAL CHARACTERIZATION

Differential Scanning Calorimetry (DSC) in a Mettler-Toledo DSC mod. 821 (Schwerzenbach, Switzerland) technique was employed to determine glass transition temperature (Tg) and melting temperature (Tm) values for the PLA in order to evaluate the extruder temperature range suggested by the provider (190 – 220 ºC). The used samples had a weight in the 5-7 mg range. The thermal transitions were evaluated in a nitrogen atmosphere with a flow rate of 66 mL min^{-1} using a dynamic temperature program according the following sequence: 1

- 1st – Heating cycle from 30 ºC to 200 ºC at 10 ºC min^{-1}
- 2nd – Cooling cycle from 200 ºC to 0 ºC at -10 ºC min^{-1}
- 3rd – Heating cycle from 0 ºC to 350 ºC at 10 ºC min^{-1}

Form of supply	Coil
Weight of coil	750 g
Diameter	2.85 mm
Maximum roundness deviation	0.03 mm
Density	1.24 g cm^{-3}
Processing temperature range	190-220 ºC

Table I. PLA material characteristics

2.3. SAMPLE MODELLING

The PLA filaments were fed into a commercial FDM desktop printer model Sigmax supplied by BCN3D (Barcelona, Spain) which extrudes the material through a 4 mm nozzle onto a heated glass bed. The parameters applied during the FDM process are numerous and they may affect the properties and the print quality of the printed samples [27]. Thus, the printing parameters applied in the present work (Table II) were kept constant for all the printed samples.

Nozzle temperature	210 ºC
Bed temperature	40 ºC
First layer height	0.3 mm
Layer height	0.1 mm
Shell thickness	1.2 mm
Outline direction	60 mm/s
Printing speed	35 mm/s
Outline underspeed	200 mm/s

Table II. FDM parameters

FreeCAD software [28], facilitated the development of the CAD data of the specimens. Then, Slic3r software [29] was used to slice the model in layers and generate a numerical control program based in G-code, Slic3r was chosen because it provides many customization options for infill patterns in comparison to other soft-

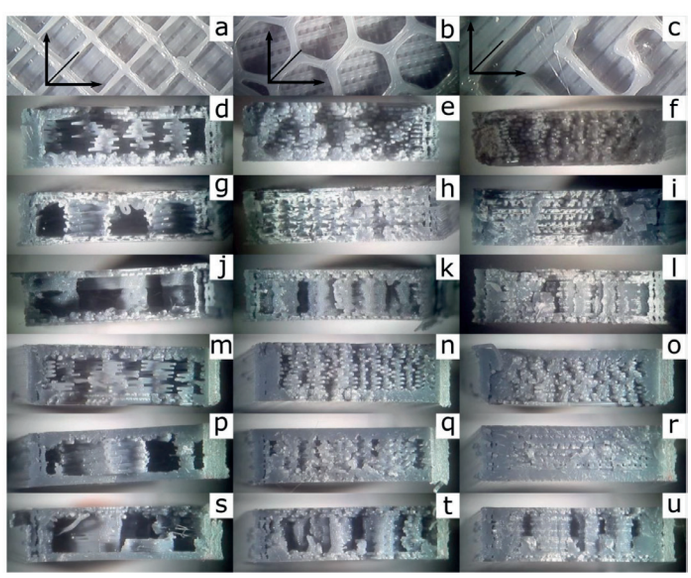

Fig. 1. Optical (8×) images. a-c images of filling patterns (20%). a) rectilinear, b) honeycomb, c) Hilbert.
d-l images of fractured samples from tensile test. d) rectilinear 20%, e) rectilinear 60%, f) rectilinear 90%, g) honeycomb 20%, h) honeycomb 60%, i) honeycomb 90%, j) Hilbert 20%, k) Hilbert 60%, l) Hilbert 90%.
m-v images of fractured samples from impact tests. m) rectilinear 20%, n) rectilinear 60%, o) rectilinear 90%, p) honeycomb 20%, q) honeycomb 60%, r) honeycomb 90%, s) Hilbert 20%, t) Hilbert 60%, u) Hilbert 90%

ware. The specimens were simulated in Repetier-Host software [30] before printing.

The specimens were printed with three different filling patterns of the most common in 3D printing, rectilinear, honeycomb and Hilbert curve. The infill percentage also was varied in order to outline its effect on mechanical properties. The specimens were printed with infills percentages of 20, 60 and 90%. However, rectilinear pattern was used for the outer surface of all the printed samples. The test specimens to be printed are rectangular shaped with dimensions of 78.5 × 18 × 5 mm. Figure 1 shows the three different infill patterns of the studied samples with 20% infill percentage and at the bottom of all of them the straight pattern of the outer face can be seen. The specimens have a rectilinear pattern on the outer surface that does not allow observation of the inside of the piece. So, the printing process was stopped once a layer of filler had been laid in order to observe the morphology of the infill (Figure 1). It should be noted that the three patterns studied present a priority orientation at 45 degrees from the main axes that would be located at the edges of the specimen.

2.4. MECHANICAL CHARACTERIZATION

At the moment, the specific mechanical characterization of polymer parts manufactured by AM is not yet standardized [31-33], so test were done using standard characterization procedures. The tensile tests were performed using a universal test machine Ibertest ELIB 30 [34] which is equipped with a 5 kN load cell. In order to minimize the randomness of the results at least five different samples were tested, and the most relevant properties were averaged. A constant crosshead speed of 5 mm min^{-1} was applied in the tensile tests in order to obtain the tensile modulus, tensile strength and the elongation at break.

The impact strength was obtained using a 1 J Charpy's pendulum supplied by Metrotec (San Sebastian, Spain) on 3D printed samples.

Dynamic-Mechanical Thermal Analysis (DMTA) tests were conducted using AR-G2 oscillatory rheometer Supplied by TA Instruments (New Castle, DE, USA) equipped with a special clamp system for solid samples which works in a combined shear-torsion mode. The samples used in the DMTA tests were scaled to 50% compared to those used in the previous tests. They were subjected to a temperature sweep from 30 °C to 140 °C at 2 °C min^{-1} under a maximum deformation (%γ) of 0.1%. Both the storage modulus (G') and the dynamic damping factor (δ) were collected using a frequency of 1Hz.

2.5. OPTICAL MICROSCOPY

In order to obtain enlarged images of the test specimen after break in the tensile and Charpy tests, an Olympus SZX7 microscope supplied by Olympus Spain, S.A.U. (Barcelona, Spain) with a magnification range of 0.8x to 5.6x was used, which is multiplied by the 10x eyepiece magnification. The microscope is equipped with a lighting equipment Olympus model KL 1500 LCD. An Olympus C-5060 wide zoom digital SLR camera was attached to the top of the magnifying glass to capture the images.

3. RESULTS

Prior to manufacture all the studied samples, the raw material was thermally characterized employing DSC technique in order to analyze both the suitability of the proposed material and the of the range of temperatures proposed by the supplier. Figure 2 shows the DSC program for raw PLA for the third step of the proposed sequence, since the first two were to eliminate the thermal history of the sample. A step is observed in the baseline at about 60-70 °C which corresponds to the glass transition temperature (*Tg*). The value of the *Tg* is determined taking the inflexion point, obtaining a value of 63.3 °C . At 105.67 °C, the DSC curve presents an exothermic peak related to the reordering of the polymer chain produced by the cold crystallization process. There is another peak at 170.36 °C, but in this case, it is endothermic, it corresponds to the melting temperature (*Tm*) of the PLA. Then, from 328.82°C there is an abrupt endothermic fall that indicates the degradation of the PLA. Thus, the thermal analysis indicates that the suggested extruder temperature range suggested by the provider (190 – 220 °C) is suitable to manufacture the planned samples since it is between the melting and the degradation and therefore it ensures that the PLA will be in molten state.

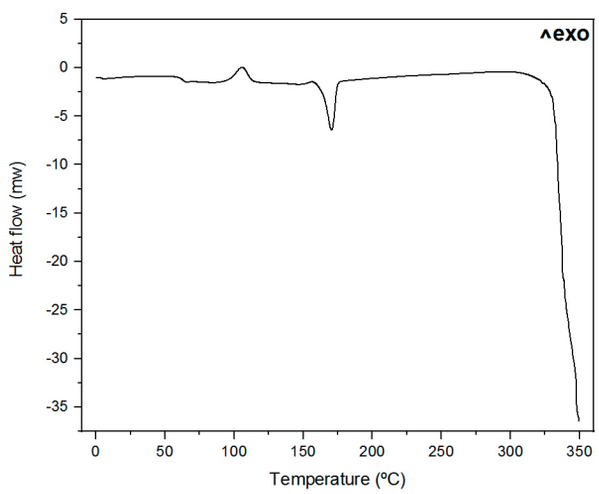

Fig. 2. DSC thermograms for raw PLA

The average weight of the 9 different types of specimens is shown in Figure 3. It is observed that there are weight differences between the different patterns studied for the same infill percentage, these differences are more pronounced when the percentages are lower and decrease as the filling increases. The honeycomb pattern has the highest weight for all concentrations. For the concentrations of 20% and 60% honeycomb pattern is followed by the rectilinear pattern and the Hilbert pattern is in last position, however for the 90% filling percentage the Hilbert pattern presents values closer to the honeycomb pattern. The Hilbert pattern shows a linear increase in weight as the percentage of filling increases. This is not the case for the other two patterns. The increase between the 60% and 90% filling percentages is less sloped than when it increases between 20% and 60%. This is due to the geometry of the patterns.

Figure 3 also depicts the printing times for the studied samples, these processing times represented were obtained from Repetier-Host simulation software. The evolution of the processing time as function of the infill percentage for all the patterns is almost linear with a gradual increase of time as infill percentage rises. As infill percentage varies from 20% to 60% the processing time increases by 55%, and if it varies to 90% the time increases by 40% more. The processing time is more dependent on the pattern used than on the amount of material used in printing. The pattern with the simplest geometry, the rectilinear one, is the one that has the lowest processing times for all the infill percentages, even though it is not the one with the least mass. This is due to the fact that the print head only moves in a straight line and does

not make direction changes that lengthen the time. Therefore, the rectilinear pattern is the most recommended from a point of view of time efficiency. On the other hand, the honeycomb pattern is the one that spends the most time due to its hexagonal geometry.

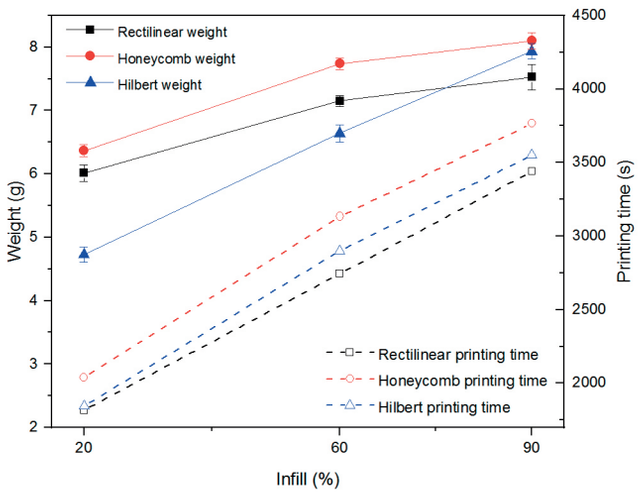

Fig. 3. Plot evolution of weight and printing time for different filling patterns as function of their infill percentage

The tensile modulus and strength values obtained in the tensile test are depicted in figure 4. As aforementioned, the investigated values were three different filling patterns and three different levels of infill percentage (20%, 60% and 90%). Analyzing the results, it can be seen that some trends have been developed when studied parameters are varied. At every filling pattern, the tensile modulus always increased with the growth in the infill percentage which indicates that increasing the infill percentage raises the rigidity of the parts. There is a direct relationship between this resistant characteristic and the amount of material, since its curves present the same tendencies as the weight ones. The honeycomb pattern is the one with the highest values of tensile modulus, except for fillings of 90% that are slightly surpassed by the rectilinear pattern. For infill percentages of 20% there is a difference of 224.64 MPa between the highest value of tensile modulus (honeycomb) and the lowest value (Hilbert). In contrast, for fillings of 90% the difference between the extreme values is reduced to 69.14 MPa. That is, the difference between the extreme values of tensile modulus decreases as the fill percentage increases. This indicates that the filling pattern is very important on the tensile modulus for low infill values, but its influence is diluted by increasing the percentage of infill. The variation of the infill percentage from 20% to 90% causes the value of the tensile modulus to increase by approximately 200% for the Hilbert pattern, while for the rectilinear pattern is 60% and for the honeycomb in a 18%.

Figure 4 also shows the evolution of the tensile strength values of the tested specimens. For tensile strength an increasing tendency is observed with the increase of infill as it happened with the tensile modulus. It is observed that the infill pattern also influences the values of tensile strength. Honeycomb remains as the pattern with the best mechanical results for all filling levels and the rectilinear shows the lowest values. The tensile modulus for the honeycomb pattern for the different infill percentages studied increases very slightly. By increasing the percentage of filling from 60% to 90%, the increase in tensile modulus is practically negligible (7.35 MPa), which indicates that as the percentage of infill increases, the tensile modulus tends to stabilize. Therefore, if the parameter of interest is the tensile modulus, the honeycomb pattern should be chosen with low infill percentages in order to save material. The tensile strength shows a slight increasing trend for the three patterns studied, with the best values being the honeycomb pattern. This increase in tensile strength values with the increase in the percentage of infill is produced by the increase in material. The honeycomb pattern, thanks to its good cohesion and load distribution, shows a linear increase, while the Hilbert pattern does not show this effect.

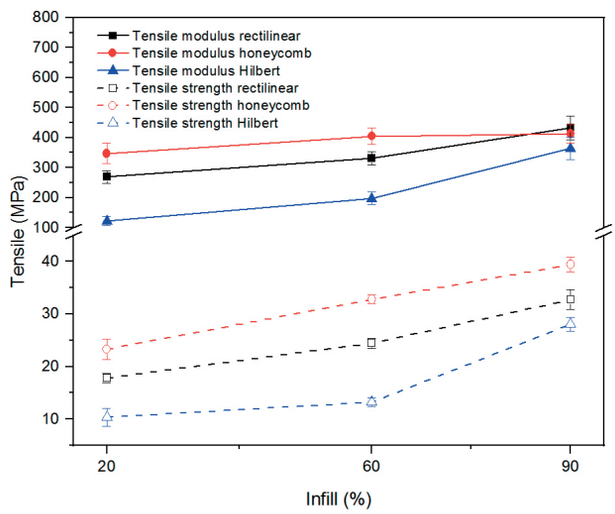

Fig. 4. Plot evolution of tensile modulus and tensile strength for different filling patterns as function of their infill percentage

Figure 5 shows the evolution of the elongation obtained in the tensile tests for the different filling patterns as function of the infill percentage. PLA presents low elongation at break values due to the brittleness nature of the material, in addition in the test pieces under study the elongation values are reduced as a consequence of the discontinuities produced by the FDM manufacturing process. These discontinuities are reduced as the infill percentage increases, regardless of the filling pattern used. Further, the Hilbert pattern presents the worst values of elongation with values that are one third of those that are obtained in pattern with the best result. The honeycomb pattern does not maintain a linear growth trend like the other two, for infill values above 60% there is a more pronounced improvement in elongation. Therefore, it is verified that for the honeycomb pattern in values of infill to

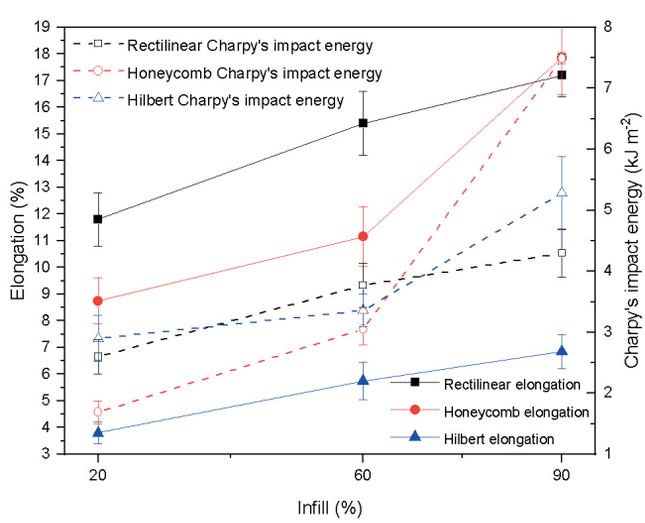

Fig. 5. Plot evolution of elongation and Charpy's impact energy absorbed for different filling patterns as function of the infill percentage

90%, elongations superior to the rectilinear pattern are obtained and altogether for high values of infill as a result of its internal structure.

Figure 1 also provides the fractured images from tensile tests. For the three patterns, it can be seen that as the infill percentage increases the size of the hollows produced by the patterns decreases. In spite of this, in all the specimens it is observed that the fracture is of a fragile character since the hollows act as stress concentrators. There is not a good transmission of internal forces as shown by the low elongation values obtained.

The intrinsic brittleness of PLA combined with the internal hollows of the test specimens produced as application of the infill pattern during the manufacturing process leads to a low toughness. In this work, the toughness has been determined using the Charpy impact test, as summarized in Figure 5. The low impact values obtained are a consequence of the notch that previously was made to the samples. For all the studied patterns, it is observed that ductility increases when the percentage of infill increases, this is due to the fact that the samples increase their mass and also the internal hollows are reduced. Furthermore, it is not observed any influence of the pattern on toughness since for the three infill values studied there is no predominant pattern nor worse. The behavior of the honeycomb pattern for the energy absorbed in the Charpy test confirms the performance shown for elongation. Since materials that have high elongation values also absorb more energy.

Figure 1 also presents the fracture images of the samples after the impact tests. The standard machined notch used to carry out the tests can be seen at the right side of the test pieces. At the opposite end of the specimen there is no plastic deformation, which indicates the fragile type of the fracture. The three patterns with low fill percentages have very large hollows that are reduced by increasing the fill percentage. The hollows act as stress concentrators, causing the material to absorb less energy on impact. For high infill percentages, the hollows are smaller, which causes better impact behavior as shown by the results.

The dynamic mechanical analysis (DMA torsion mode) of the samples filled with honeycomb pattern is shown in figure 6. This analysis can be applied to the other two patterns, since they present the same behavior. Figure 6 shows the evolution of the storage module (G') for the samples with honeycomb pattern with the three different infill levels as a function of temperature. In the curves four different stages are observed, the first stage is below the glass transition temperature (Tg) ranged 30-50 ºC. As one can see, the initial storage modulus increases as the infill percentage increases with values of 1,007 MPa, 1,160 MPa and 12,179 MPa at 40 ºC for samples containing 20%, 60% and 90% infill respectively indicating stiffer materials as pointed in previous analysis. In the range of 50-70 ºC a softening of the material occurs; this phenomenon causes the G' module to be reduced by more than two orders of magnitude. The decrease is proportional to the amount of material in the sample. In this range, the vitreous transition of the material occurs, which confirms the temperature obtained with the DSC test. The G' values at 70 °C are 8.86 MPa, 5.24 MPa and 3.88 MPa for samples containing 20%, 60% and 90% filler respectively. The third stage ranges between 70 ºC and 90 ºC, in it the PLA undergoes a cold crystallization process. The PLA analyzed had previously suffered a cooling after the 3D printing process, but it was not able to full crystallize since this process requires more time or temperature. When the temperature exceeds 70 ºC, the necessary energy is provided to the material, so the PLA chains begin to move and pack resulting in an increase in crystallinity. By increasing the crystallinity, the material becomes stiffer as shown in the graph with a growth of G' in an order of magnitude. Once the crystallization process is finished, the storage module behaves similarly to the first stage, with maximum values for the samples with the highest infill percentage (90%) with values of 86.30 MPa at a temperature of 100 ºC, while the samples with infills of 20% and 60% reach values of 69.06 MPa and 81.46 MPa respectively.

In Figure 6 the variation of the damping factor (Tan δ) as a function of temperature is also depicted. If the maximum peak of Tan δ is considered as a representative value of the Tg, values of 62.7 ºC, 63.4 ºC and 63.7 ºC are obtained for the samples containing 20%, 60% and 90% infill respectively. These values are very similar among them and with the value obtained in the DSC test (63.3 ºC) since Tg is an intrinsic property of the material and practically does not depend on the cohesion or geometry of the 3D print. What stands out in figure 6 are the decreasing values of Tan δ as the infill percentage increases. This trend is logical, as the material becomes stiffer the value of G' increases, which causes smaller losses. In fact, for the sample with 20% honeycomb the maximum value of Tan δ is 1.64 and this value is reduced to 1.12 for the 90% honeycomb sample.

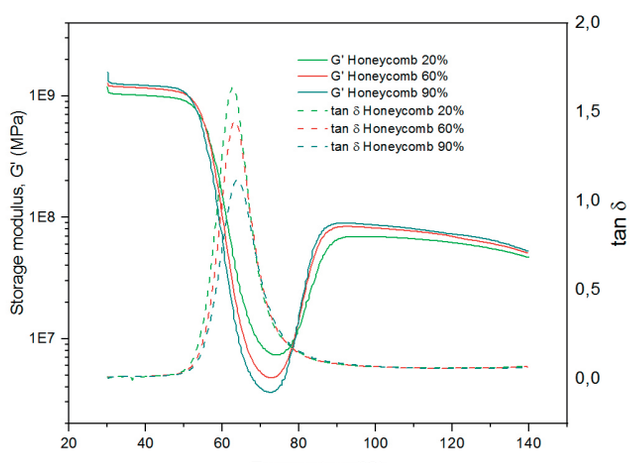

Fig. 6: Storage modulus (G') and damping factor (Tan δ) of honeycomb filled samples as a function of temperature

4. CONCLUSIONS

The effects of the infill pattern and percentage on the mechanical properties of PLA polymer specimens processed by FDM or material extrusion additive manufacturing were studied. The manufacture of the specimens was controlled so that external factors such as humidity do not affect the results. Specimens were tested with three different infill patterns and with three different infill percentages. Tensile, impact and themomechanical properties were examined in order to compare all levels with each other and the following results were obtained:

- The rectilinear pattern is the most recommended from a time efficiency point of view.
- Printing time is more dependent on the pattern used than on the amount of material used. As the complexity of the pattern increases, so does the processing time.
- The influence of the infill pattern on tensile values is significant for low infill percentage values but dilutes as the % infill increases. As the percentage load increases, the tensile characteristics among the three studied patterns become similar. So, for low filler percentages it is advisable to use the

honeycomb pattern and avoid the rectilinear pattern in order to achieve better mechanical characteristics.

- The intrinsic brittleness of the polymeric material used, PLA, combined with the discontinuities produced by the hollows of the patterns drag down the mechanical results since they act as stress concentrators and do not allow a correct transmission of internal forces.

REFERENCES

[1] Masood SH "Intelligent rapid prototyping with fused deposition modelling". Rapid Prototyping Journal. Vol.2-1 p.24-33. DOI: http://dx.doi.org/10.1108/13552549610109054
[2] Gordelier TJ, Thies PR, Turner L, et al. "Optimising the FDM additive manufacturing process to achieve maximum tensile strength: a state-of-the-art review". Rapid Prototyping Journal. Vol.25-6 p.953-971. DOI: http://dx.doi.org/10.1108/rpj-07-2018-0183
[3] Attaran M "The rise of 3-D printing: The advantages of additive manufacturing over traditional manufacturing". Business Horizons. Vol.60-5 p.677-688. DOI: http://dx.doi.org/10.1016/j.bushor.2017.05.011
[4] Berman B "3-D printing: The new industrial revolution". Business Horizons. Vol.55-2 p.155-162. DOI: http://dx.doi.org/10.1016/j.bushor.2011.11.003
[5] Despeisse M, Ford S, The Role of Additive Manufacturing in Improving Resource Efficiency and Sustainability, in Advances in Production Management Systems: Innovative Production Management Towards Sustainable Growth, S. Umeda, M. Nakano, H. Mizuyama, et al., Editors. 2015. p. 129-136.
[6] Gao W, Zhang Y, Ramanujan D, et al. "The status, challenges, and future of additive manufacturing in engineering". Computer-Aided Design. Vol.69-p.65-89. DOI: http://dx.doi.org/10.1016/j.cad.2015.04.001
[7] Barrios-Muriel J, Romero-Sanchez F, Alonso-Sanchez FJ, et al. "Application of technologies of rapid prototyping in the fabrication of orthoprosthetic devices". DYNA. Vol.91-4 p.381-385. DOI: http://dx.doi.org/10.6036/7784
[8] Stansbury JW, Idacavage MJ "3D printing with polymers: Challenges among expanding options and opportunities". Dental Materials. Vol.32-1 p.54-64. DOI: http://dx.doi.org/10.1016/j.dental.2015.09.018
[9] Grémare A, Guduric V, Bareille R, et al. "Characterization of printed PLA scaffolds for bone tissue engineering". Journal of Biomedical Materials Research Part A. Vol.106-4 p.887-894. DOI: http://dx.doi.org/10.1002/jbm.a.36289
[10] Guerra AJ, Cano P, Rabionet M, et al. "3D-Printed PCL/PLA Composite Stents: Towards a New Solution to Cardiovascular Problems". Materials. Vol.11-9 DOI: http://dx.doi.org/10.3390/ma11091679
[11] Dawoud M, Taha I, Ebeid SJ "Mechanical behaviour of ABS: An experimental study using FDM and injection moulding techniques". Journal of Manufacturing Processes. Vol.21-p.39-45. DOI: http://dx.doi.org/10.1016/j.jmapro.2015.11.002
[12] Goh GD, Agarwala S, Goh GL, et al. "Additive manufacturing in unmanned aerial vehicles (UAVs): Challenges and potential". Aerospace Science and Technology. Vol.63-p.140-151. DOI: http://dx.doi.org/10.1016/j.ast.2016.12.019
[13] Mohamed OA, Masood SH, Bhowmik JL "Optimization of fused deposition modeling process parameters: a review of current research and future prospects". Advances in Manufacturing. Vol.3-1 p.42-53. DOI: http://dx.doi.org/10.1007/s40436-014-0097-7
[14] Casavola C, Cazzato A, Moramarco V, et al. "Orthotropic mechanical properties of fused deposition modelling parts described by classical laminate theory". Materials & Design. Vol.90-p.453-458. DOI: http://dx.doi.org/10.1016/j.matdes.2015.11.009
[15] Ulu E, Korkmaz E, Yay K, et al. "Enhancing the Structural Performance of Additively Manufactured Objects Through Build Orientation Optimization". Journal of Mechanical Design. Vol.137-11 DOI: http://dx.doi.org/10.1115/1.4030998
[16] Domingos M, Chiellini F, Gloria A, et al. "Effect of process parameters on the morphological and mechanical properties of 3D bioextruded poly (ε-caprolactone) scaffolds". Rapid Prototyping Journal. Vol.18-1 p.56-67. DOI: http://dx.doi.org/10.1108/13552541211193502
[17] Araya-Calvo M, Lopez-Gomez I, Chamberlain-Simon N, et al. "Evaluation of compressive and flexural properties of continuous fiber fabrication additive manufacturing technology". Additive Manufacturing. Vol.22-p.157-164. DOI: http://dx.doi.org/10.1016/j.addma.2018.05.007
[18] Boyard N, Christmann O, Rivette M, et al. "Support optimization for additive manufacturing: application to FDM". Rapid Prototyping Journal. Vol.24-1 p.69-79. DOI: http://dx.doi.org/10.1108/RPJ-04-2016-0055
[19] Yosofi M, Kerbrat O, Mognol P "Framework to Combine Technical, Economic and Environmental Points of View of Additive Manufacturing Processes". Procedia CIRP. Vol.69-p.118-123. DOI: http://dx.doi.org/10.1016/j.procir.2017.11.085
[20] Yang C, Tian X, Liu T, et al. "3D printing for continuous fiber reinforced thermoplastic composites: mechanism and performance". Rapid Prototyping Journal. Vol.23-1 p.209-215. DOI: http://dx.doi.org/10.1108/RPJ-08-2015-0098
[21] Torres J, Cotelo J, Karl J, et al. "Mechanical property optimization of FDM PLA in shear with multiple objectives". JOM. Vol.67-5 p.1183-1193. DOI: http://dx.doi.org/10.1007/s11837-015-1367-y
[22] Tymrak B, Kreiger M, Pearce JM "Mechanical properties of components fabricated with open-source 3-D printers under realistic environmental conditions". Materials & Design. Vol.58-p.242-246. DOI: http://dx.doi.org/10.1016/j.matdes.2014.02.038
[23] Vaezi M, Chua CK "Effects of layer thickness and binder saturation level parameters on 3D printing process". International Journal of Advanced Manufacturing Technology. Vol.53-1-4 p.275-284. DOI: http://dx.doi.org/10.1007/s00170-010-2821-1
[24] Rodríguez-Panes A, Claver J, Camacho A "The Influence of Manufacturing Parameters on the Mechanical Behaviour of PLA and ABS Pieces Manufactured by FDM: A Comparative Analysis". Materials. Vol.11-8 p.1333. DOI: http://dx.doi.org/10.3390/ma11081333
[25] Wu W, Geng P, Li G, et al. "Influence of Layer Thickness and Raster Angle on the Mechanical Properties of 3D-Printed PEEK and a Comparative Mechanical Study between PEEK and ABS". Materials. Vol.8-9 p.5834-5846. DOI: http://dx.doi.org/10.3390/ma8095271
[26] Valerga A, Batista M, Salguero J, et al. "Influence of PLA Filament Conditions on Characteristics of FDM Parts". Materials. Vol.11-8 p.1322. DOI: http://dx.doi.org/10.3390/ma11081322
[27] Bellehumeur C, Li L, Sun Q, et al. "Modeling of bond formation between polymer filaments in the fused deposition modeling process". Journal of Manufacturing Processes. Vol.6-2 p.170-178. DOI: http://dx.doi.org/10.1016/S1526-6125(04)70071-7
[28] FreeCAD software, release 0.18. Available from: https://www.freecadweb.org/.
[29 Slic3r software release 1.3.0. Available from: http://slic3r.org/.
[30] Repetier-Host software, release 2.1.6. Available from: https://www.repetier.com/.
[31] Slotwinski JA. Mechanical Properties of Materials Made Via Additive Manufacturing. ASTM Standardization News [On-line article] 2013; Available from: https://www.astm.org/standardization-news/?q=update/mechanical-properties-of-materials-made-via-additive-manufacturing-nd13.html
[32] Forster A "Materials testing standards for additive manufacturing of polymer materials". NI:ST, Department of Commerce. Vol.8059-
[33] Monzon MD, Ortega Z, Martinez A, et al. "Standardization in additive manufacturing: activities carried out by international organizations and projects". International Journal of Advanced Manufacturing Technology. Vol.76-5-8 p.1111-1121. DOI: http://dx.doi.org/10.1007/s00170-014-6334-1
[34] Ibertest ELIB 30. Supplied by S.A.E. Ibertest (Madrid, Spain).

ACKNOWLEDGMENTS

This work was supported by the POLISABIO program grant number (2019-A02). J. Ivorra-Martinez wants to thank UPV for the grant received through the FPI program, grant (SP20190011). L. Quiles-Carrillo wants to thank MECD for his FPU grant (FPU15/03812). D. Lascano wants to thank UPV for the grant received through the PAID-01-18 program.